Articles

Potential Energy Surface from Spectroscopic Data in the Photodissociation of Polyatomic Molecules

Hwa Joong Kim and Young Sik Kim[†,*]

Department of Chemical Engineering, [†]Department of Basic Science, Hong-ik University, Seoul 121-791, Korea
Received October 27, 2000

The time-dependent tracking inversion method is studied to extract the potential energy surface of the electronic excited state in the photodissociation of triatomic molecules. Based on the relay of the regularized inversion procedure and time-dependent wave packet propagation, the algorithm extracts the underlying potential energy surface piece by piece by tracking the time-dependent data, which can be synthesized from Raman excitation profiles. We have demonstrated the algorithm to extract the potential energy surface of electronic excited state for NO_2 molecule where the wave packet split on a saddle-shaped surface. Finally, we describe the merits of the time-dependent tracking inversion method compared with the time-independent inversion method and discussed several extensions of the algorithm.

Keywords : Potential energy surface, Wave packet propagation, Inversion method, Photodissociation dynamics, Raman spectra.

Introduction

The dissociation of molecules through the absorption of UV photons is the most fundamental problem of photochemistry and chemical processes. This phenomenon is well suited for the study of intra- and intermolecular dynamics, coupling among different bonds, energy transfer from one mode to the others, the breaking of bonds and the formation of new ones. During the last two decades, the improving state of the art of crossed-beam techniques in combination with ultrashort laser pulses and high-resolution spectroscopic techniques has provided details of photodissociation processes in polyatomic molecules. Complete identification of the initial state in the ground state and dynamics calculations for the excited state surfaces enable researchers to obtain a sequence of snapshots of a molecular system from its preparation all the way through to the product.

Using highly successful modern experimental techniques, theoreticians have greatly advanced computational methods to treat photodissociation processes. The power of modern computers allows access to the dissociation dynamics of triatomic molecules by exact quantum mechanical methods without any approximation. In the field of photodissociation, the close interplay between experiment and theory has contributed greatly to the understanding of photochemical processes.

However, the potential energy surface (PES) of triatomic molecules has complicated topology, especially for excited electronic states. Avoiding crossings of the PES of interest with the PES's of other electronic states can lead to potential barriers or potential wells. Also, in addition to the unique dissociation channel, there are other channels, including the breakup into three atoms. Thus, the exact information of the PES is important to the study of dissociation dynamics.[1] The determination of PES has been studied for many years by two different approaches.[2-4] One approach is to perform *ab initio* calculation's within the Born-Oppenheimer approximation,[5] which is a forward method, and the other, which is an inverse method,[6-8] is to perform inversion of experimental data.

In recent years, *ab initio* calculations have been very advanced but still limited to relatively small systems and lacking the accuracy demanded by quantitative dynamical calculation. Most of existing numerical procedures to extract PES from laboratory data use a traditional least-squares fitting methods,[9] but these methods have the drawback of constraining PES's to follow a fixed function form, making good fits difficult to obtain. Without the assumption of any PES form, a direct inversion method is available for the simple case of diatomic molecules. It is known as the semi-classical Rydberg-Klein-Rees (RKR) method.[10] Although the RKR method has been used successfully to determine of one-dimensional PES, it cannot be applied to replusive PES's and to a PES with more than one minimum.[11]

Recently, a regularized inversion method was developed within the framework of the Tikhonov regularization procedure.[12] The method is related to the iterative inversion algorithm, which extracts the underlying PES, based on the functional derivatives of the experimental data with respect to the PES. One important aspect of this method is that it allows the value of the PES at every point in space to vary independently compared with the parameter-fitting methods. Because there are more discretization points for PES than data points (*i.e.*, ill-posedness of the inversion[12-16]), reasonable regularization constraints have to be included for the stability of the

solution, e.g., smoothness of the potential.

In general, experimental data can be obtained from either stationary (frequency-domain)[7-8] or time-dependent experiments. The latter just recently became available as exciting real-time dynamical experiments, such as femtosecond transition-state spectroscopy (FTS).[17-22] Both frequency-domain and time-dependent measurements can reflect the same basic information about the molecules involved.[20] Gruebele *et al.*[21] have reported on the use of FTS to yield accurate spectral information (vibrational and rotational) via Fourier transformation and to directly invert to the PES, using the semiclassical RKR method. (*i.e.*, frequency-domain inversion).[23]

In the present study, we expand our earlier time-dependent tracking inversion method to systems with more than one internal degree of freedom. This method applies to the triatomic system to extract PES of the electronic excited state from tracking the time-dependent data[24] (*i.e.* the correlation function) which can be synthesized from frequency-domain measurements, such as the Raman excitation profile (REP) in photodissociation processes. The merits of the time-dependent tracking inversion method[24] are as following; First, there is no need to assign energy level labels. In polyatomic molecules, this task is notoriously difficult in the frequency-domain inversion approach. However, the assignment problem is completely avoided in the tracking algorithm, since the time ordering of data does the assigning. Second, compared with the iterative inversion method in frequency domain, the proposed inversion algorithm is direct and computationally efficient because it solves the inversion problem at each time step extracting the PES piece by piece.

In the following section, we outline the time-dependent inversion method based on the Tikhonov regularization procedure to extract the PES from the correlation function. Next, we simulate the inversion of the PES of the excited electronic state of NO_2 where the wave packet split on a saddle-shaped surface from the REP in photodissociation processes. This is followed by discussions on possible applications of the inversion method to problems involving the dipole function and the PES, simultaneously.

Theory

Figure 1 shows the photodissociation of a triatomic molecule *ABC* into products *A* and *BC*. Before the absorption process, the molecule is assumed to be in a particular initial vibrational state $|\phi_i\rangle$ in the ground electronic state (S_0). Absorption of a photon promotes a molecule to the excited electronic state (S_1) on which the initial wave packet $|\psi(0)\rangle$ is propagated, according to the time-dependent schrödinger's equation. The corresponding PES's will be denoted by V_g and V_e, respectively. If the upper-state potential is purely repulsive along the dissociation coordinate R, the molecule dissociates immediately into the fragments $A+BC$. If, on the other hand, V_e has a barrier that blocks direct dissociation, the bond dissociation will be delayed.

When molecules are excited to a photodissociative continuum, the absorption spectrum $\sigma_{abs}(w)$ measures the proba-
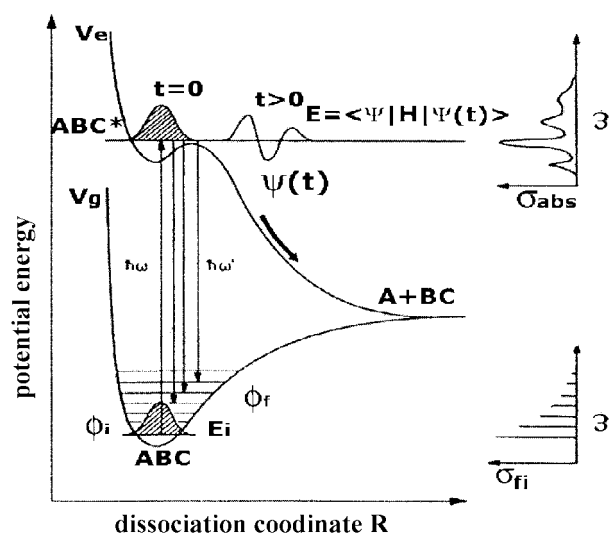

Figure 1. The UV photodissociation of triatomic molecule ABC into products A+BC. The electronic excitation occurs from the molecule in a particular initial state $|\phi_i\rangle$ in the ground electronic state (S_0) to the excited singlet electronic state (S_1). The corresponding PES are V_g and V_e, respectively. $\sigma_{abs}(w)$ and $\sigma_{fi}(\omega)$ denote the absorption cross section and the Raman scattering cross section, respectively.[31]

bility of absorbing a photon with specific frequency irrespective of the fate of the excited molecule. It depends primarily on the shape of the PES in the Franck-Condon (FC) region. The vast majority of excited molecules dissociate without any emitted radiation. A very small fraction will exchange one of the incident photons ω for one of a different wavelength ω', thereby returning to a different vibrational level of the ground electronic state $|\phi_f\rangle$. Because the lifetime of the dissociating molecule is usually less than the order of picoseconds and much shorter than the lifetime for spontaneous emission, which is of the order of nanoseconds, the intensity of the emitted light is extremely low. Nevertheless, it can be measured with sensitive detectors, and its intensity is given by the Raman scattering cross-section $\sigma_{fi}(w)$.

$$\sigma_{fi}(\omega) = \omega\omega'^3 |\alpha_{fi}(\omega)|^2, \tag{1}$$

where ω and ω' are the incident frequency and the scattered frequency, respectively.

The dependence of the cross-section for a given transition upon the excitation frequency ω will be referred to as the Raman excitation profile (REP). It reflects the motion of the dissociating complex in the excited electronic state and is used to extract information about V_e. Because the REP involves the overlap of the wave function in the upper electronic state with the excited vibrational states in the ground electronic state, it is sensitive to a wider region of the upper PES than the absorption spectrum $\sigma_{abs}(w)$. $\alpha_{fi}(\omega)$ in Eq. (1) is the polarizability appropriate to this transition and expressed as

$$\alpha_{fi}(\omega) = \int_0^\infty dt\, e^{i(\omega + E_i/\hbar + i\Gamma)t} S_{fi}(t), \tag{2}$$

where E_i is the energy of the initial vibrational state and Γ is the usual phenomenological damping parameter (*i.e.*, the inverse of the lifetime). $S_{fi}(t)$ is the correlation function defined as

$$S_{fi}(t) = \langle \phi_f | \mu e^{-iH_e t/\hbar} \mu | \phi_i \rangle, \qquad (3)$$

where H_e is the nuclear Hamiltonian in the excited electronic state, and μ represents the transition dipole moment.

For simplicity, we assume that the ground electronic state is understood so well that its vibrational eigenfunctions and energies are available. Then, with the knowledge of the excited electronic state's PES, V_e and the transition dipole moment μ, it is straightforward to calculate the REP for every possible transition given in Eqs (2) and (3). However, is it possible to get the information about V_e from the REP's.

With the known initial wave packet and the correlation function, which can be obtained from the REP, we want to extract the PES of the excited electronic state on which the wave packet is propagated. In the limit of the Condon approximation (to ignore dependence of the transition moments on internal nuclear coordinates), the initial non-stationary wave packet on the excited PES in the FC region can be prepared as $|\phi_i \rangle = |\psi_i(0)\rangle$, and the initial wave packet is propagated on the excited PES according to the time-dependent Schrödinger's equation. The solution can be expressed as $e^{-iH_e t/\hbar}|\phi_i(0)\rangle = |\psi_i(t)\rangle$. Then, Eq. (3) can be rewritten as following

$$S_{fi}(t) = \langle \phi_f | \psi_i(t) \rangle. \qquad (4)$$

Further differentiating $S_{fi}(t)$ with respect to t, the PES of the excited state can be related to it as

$$i\hbar \frac{dS_{fi}(t)}{dt} = \left\langle \phi_f \left| i\hbar \frac{d}{dt} \right| \psi_i(t) \right\rangle$$
$$= \langle \phi_f | T | \psi_i(t) \rangle + \langle \phi_f | V_e | \psi_i(t) \rangle, \qquad (5)$$

where the Hamiltonian of the excited electronic state is partitioned into kinetic and potential operators $H_e = T + V_e$. The time derivative of the correlation function and the kinetic energy operator T is known and the potential V_e is what we want to extract. Rearranging Eq. (5) gives the Fredholm integral equation of the first kind as

$$\int_0^\infty \vec{dR} K_f(\vec{R}, t) f(\vec{R}) \vec{R}^2 = g_f(t), \qquad (6)$$

where the known term $g_j(t)$ and the kernel $K_j(\vec{R}, t)$ in Eq. (6) are

$$g_f(t) = i\hbar \frac{dS_{fi}(t)}{dt} - \langle \phi_f | T | \psi_i(t) \rangle; \quad f(\vec{R}) = V_e \qquad (7)$$

$$K_f(\vec{R}, t) = \phi_f^*(\vec{R}) \psi_i(\vec{R}, t) / \vec{R}^2. \qquad (8)$$

If we put $t = 0$ in Eq. (5), the solution of the integral equation gives the local excited potential V_e^0, where the initial non-stationary states $\psi_j(0)$ are localized in the FC region.

Then, this piece of potential V_e^0 is used to propagate the wave function $\psi_j(0)$ to the next time $\psi_j(t)$, according to the time-dependent schr dinger equation by the split operator method of Feit and Fleck.[27] The wave function at the next time step can be expressed as

$$|\psi_i(t)\rangle = e^{-iH_e t/\hbar} |\psi_i(0)\rangle$$
$$\approx e^{-iTt/2\hbar} e^{-iV_e t/\hbar} e^{-iTt/2\hbar} |\psi_i(0)\rangle. \qquad (9)$$

With the known ϕ_f and $\psi_i(t)$ [i.e., using the correlation function $S_{fi}(t)$], Eq. (6) gives the next piece of the potential V_e^1. With V_e^1, the wave function at the next time step $\phi_i(2t)$ can be obtained by propagation, and wave functions ϕ_f and $\psi_i(2t)$ allow obtaining V_e^2 from Eq. (8), etc. The relay of the inversion process and the wave packet propagation continue until the wave functions have sampled all dynamically accessible regions of the PES. Finally, the potential is the sum of these pieces, V_e^i.

In general, with the known PES's, the correlation function can be calculated from Eq. (4), because this forward problem is usually well-posed problem and it has a unique solution. However, the inverse problem of extracting PES from experimental data is ill-posed problem because it corresponds to the determination of the continuous PES from a given set of discrete data (observable measurements). A reasonable regularization constraint, e.g. smoothness of PES, is needed to solve Eq. (7). For this, Eq. (7) can be transformed, via integration by parts as

$$g_f = \int_0^\infty d\vec{R} K_f^{[n]}(\vec{R}) f^{(n)}(\vec{R}), \qquad (10)$$

where

$$K_f^{[n]}(\vec{R}) = -\int_0^{\vec{R}} d\vec{R}' K_f^{[n-1]}(\vec{R}'), \text{ and } f^{(n)}(\vec{R}) = \frac{d^n f(\vec{R})}{d\vec{R}^n}.$$

Here we have taken into account the fact that the potential, as well as its derivative, $V^{(n)}(\vec{R})$, usually approach zero quickly as the dissociation coordinate becomes infinite. Then, the regularized solution in Eq. (10) is achieved by minimizing the following functional[7]

$$J[f^{(n)}, g_f] = \sum_f \left| \int_0^\infty d\vec{R} K_f^{[n]}(\vec{R}) f^{(n)}(\vec{R}) - gf \right|^2$$
$$+ \alpha \int_0^\infty d\vec{R} [f^{(n)}(\vec{R})]^2. \qquad (11)$$

The regularization parameter α denotes the tradeoff between reproducing the data and obtaining a smooth solution. If we choose too small an α value, PES is overfitted with the data and lose smoothness. On the other hand, the resolution of PES may be very poor if we try to oversuppress the smoothness of PES by choosing too large an α value. Consequently, it is necessary to properly choose an α value for Eq. (11) to yield an adequate PES. The solution of Eq. (11) can be obtained by a singular value decomposition method as

$$f^{(n)} = \sum_j \frac{(u_j^T g_f)}{w_j^2 + \alpha} w_j v_j(\vec{R}),$$

where u_j, $v_j(\vec{R})$ are the singular function for the kernel K_j^T and K_j, with singular values w_j

$$\sum_j K_j^{[n]}(\vec{R}) u_{j,p} = w_p v_p(\vec{R}) \qquad (13)$$

$$\int_0^\infty d\vec{R} K_j^{[n]}(\vec{R}) v_p(\vec{R}) = w_p u_{j,p} . \qquad (14)$$

For a more detailed derivation, see Ref. 12.

Calculations

In our previous numerical study, a simple diatomic-like model was used to demonstrate the applicability of the time-dependent tracking inversion method to absorption spectra. In the present paper, we expand this method to systems with more than one internal degree of freedom. Our target molecule is NO_2.[28-36] The coordinates r_1, r_2 and θ define the dynamics for NO_2, where r_1 and r_2 denote the distances from N to each of the O atoms. The coordinate θ is the bending angle between the two radial NO directions. In these coordinates, the two-dimensional Hamiltonian for NO_2 is defined by

$$H = \frac{1}{2\mu}\left(\frac{\partial^2}{\partial r_1^2} + \frac{\partial^2}{\partial r_2^2}\right) - \frac{\cos\theta}{m_N}\frac{\partial^2}{\partial r_1 \partial r_2} + V(r_1, r_2, \theta), \quad (15)$$

where $\mu^{-1} = m_O^{-1} + m_N^{-1}$ and m_O and m_N are the masses of the oxygen and nitrogen, respectively.

The time-dependent study of NO_2 photodissociation is defined by two PES, S_0 and S_1, corresponding to the electronic ground and excited states, respectively.[29] The S_0 surface typically has a pronounced well leading to the presence of bound states. The S_1 surface may have a shallow well, which may not be able to support bound states. The S_1 surface is based on the *ab initio* data. The original expression given by Hirsch and Buenker[37] as

$$V(r_1, r_2, \theta) = V_{NO_2}(r_1) + V_{NO_2}(r_2) + [1 - Q_1(r_1)]$$

$$\times [1 - Q_a(r_2)] \sum_{k,l,m} b_{klm} Q_a(r_1)^k Q_a(r_2)^l Q_b(\theta)^m, \quad (16)$$

where

$$Q_a(r) = 1 - \exp[-\beta(r - r_{eq})] \qquad (17a)$$

$$Q_b(\theta) = \alpha_1(\theta - \theta_{eq}) + \alpha_2(\theta - \theta_{eq})^2 + \alpha_3(\theta - \theta_{eq})^3 \quad (17b)$$

$$V_{NO}(r) = a_2 Q_a(r)^2 + a_3 Q_a(r)^3 + a_4 Q_a(r)^4 . \qquad (17c)$$

All parameters are given in Ref. 31.

The ground PES is used for determining the ground state wave function to be used as the initial wave packet on the S_1 surface. For simplicity, the bending angle θ is frozen at a selected equilibrium value θ_{eq}. Using the equilibrium value $r_e = 2.27$ *a.u.*, for r_1, r_2, the ground Morse PES is given as

$$V(r_1, r_2) = D_e[1 - e^{-a(r_1 - r_2)}]^2 + D_e[1 - e^{-a(r_1 - r_e)}]^2 \quad (18)$$

and the corresponding ground state gaussian wave functions are given as

$$\phi_{n_1, n_2}(r_1, r_2) = P_{n_1}(r_1) P_{n_2}(r_2) \qquad (19a)$$

$$P_n(r) = \left[\frac{n!a(2t - 2n - 1)}{\Gamma(2t - n)}\right] \times x^{t-n-1/2} L_n^{2t-2n-1}(x) e^{-x/2}, \quad (19b)$$

where $L_n(x)$ is a Laguerre polynomial,

$$x = 2te^{-a(r - r_e)} \qquad (19c)$$

$$t = (2\mu D)^{1/2}/\hbar a . \qquad (19d)$$

These parameters in atomic unit $(D, r_e, a) = (0.2953, 2.27, 1.3164)$ can be found in Ref. 36.

To perform the wave packet dynamics calculation, the ground state wave function was first computed on the S_0 surface. This ground state wave functionvert $|\phi_i\rangle$ was vertically shifted to the S_1 surface to provide the initial wave packet propagated on the excited PES. Starting at an N-O distance of 1.6 a.u., 256 grid points were placed every 0.05 a.u. in each coordinate. It should be pointed out that in all calculations presented here the vibronic coupling between the S_0 and the S_1 surface is neglected. However, the dynamics on the isolated diabatic S_1 surface of NO_2 gives reasonable spectroscopic data and provides a significant test for the feasibility of the time-dependent tracking inversion method.

Figure 2 shows the wave packetvert $|\psi(t)\rangle$ as a function of the symmetric stretch coordinate $r_1 + r_2$ and the asymmetric stretch coordinate $r_1 - r_2$ at 0, 12, 24, 48 and 120 fs. The corresponding PES $V(r_1, r_2, \theta_0)$ of the S_1 state is given for a fixed value $\theta_{eq} = 133.89°$, which is the equilibrium bending angle in the ground state. It has been found that the wave packet spreads along the dissociation coordinate during the propagation. Initially, the compact wave packet moves in the direction of the symmetric stretch coordinate $r_1 + r_2$. Since the motion occurs on the saddle of the PES, strong spreading of the wave packet in the direction of the asymmetric stretch coordinate $r_1 - r_2$ was found. After about 24 fs, the turning point of the symmetric stretch motion is reached. The wave packet becomes extremely broad and starts moving toward the potential valleys.

The amplitude of the correlation function is shown in Figure 3. Two recurrences are apparent, one at approximately 48 fs and the other at 120 fs. The first recurrence corresponds to the symmetric stretch resonance that occurs because some portion of the wave packet is reflected from the symmetric stretch barrier and returns to the FC region. Another portion is reflected from the barrier toward the repulsive wall to the dissociation valleys. Because of the geometry of the PES, some portion is reflected back toward the barrier and then redirected back to the FC region at approximately 120 fs.

The REP $\sigma_{fi}(E)$ is obtained from Eq. (1) and (2) as the Fourier transform of the correlation function. This is shown
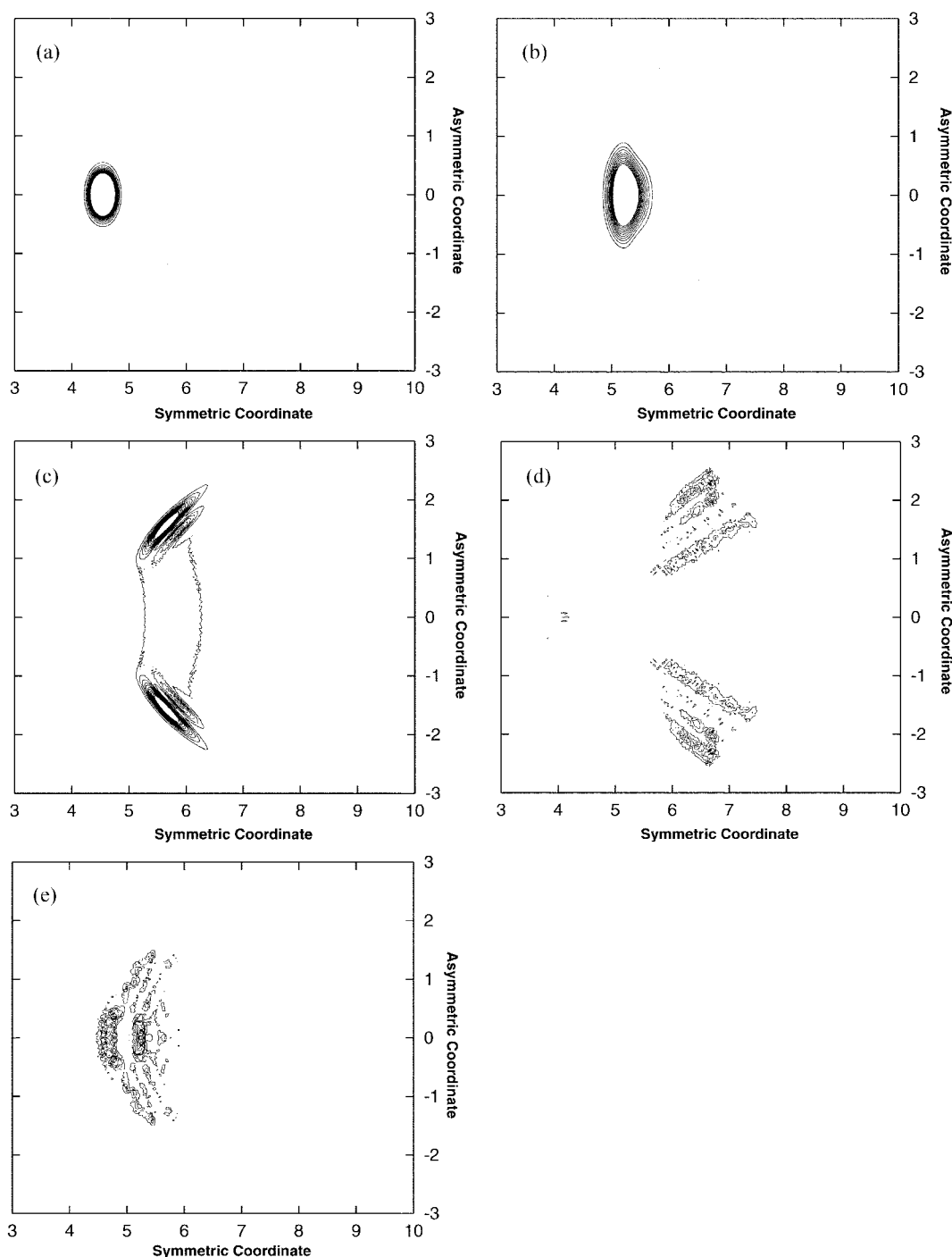
Figure 2. the wave packetvert $\psi(t) >$ as a function of the symmetric stretch coordinate $r_1 + r_2$ and asymmetric stretch coordinate $r_1 - r_2$ at (a) 0, (b) 12, (c) 24, (d) 48 and (e) 120 fs ($\theta = 133.89°$).

in Figure 4 as the solid line for $f = (0,0)$. When the final vibrational state f is the same as the initial state, the correlation function becomes the auto-correlation function and the REP becomes the absorption spectrum. The overall envelope of the absorption spectrum is controlled by the width of the correlation functions and small spikes can be explained by the oscillation period of the symmetric stretch resonance and the hyperspherical resonance.

From differentiating $S_{fi}(t)$ with respect to t and initial conditions, we have performed the relay of the inversion proce-

dure and the wave packet propagation to extract the underlying PES piece by piece. Comparisons of the inverted potentials with the exact one, according to the time evolution of the wave packet, are shown in Figure 5. In Figure 5(a), the comparison is shown along r_1 at the fixed equilibrium position ($r_2 = 2.4125$ a.u.) of S_1 surface. Figure 5(b) displays along the symmetric stretch coordinate ($r_1 + r_2$) at a fixed asymmetric stretch coordinate (i.e. $r_1 = r_2$). We found that the inversion algorithm extracts the potential beyond the FC region function, and that the inverted potential closely resembles
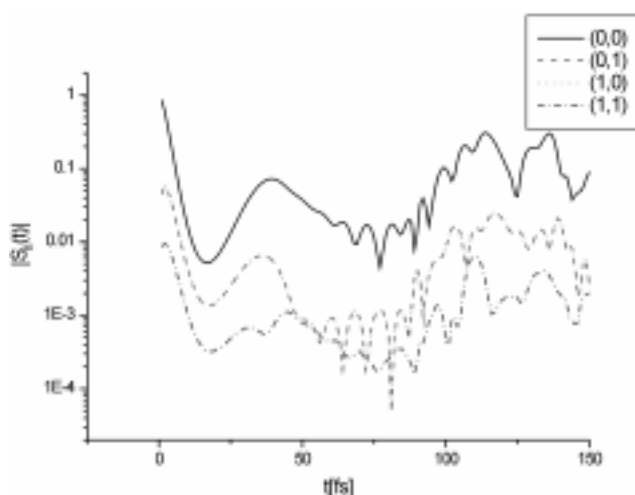
Figure 3. The amplitude of the correlation function ($\theta = 133.89°$).

the exact one until the wave packet reaches the turning point in the symmetric coordinate. Beyond the turning point, there is a sizable difference from the exact ones at the large distance where the wave packet cannot reach.

Table 1 presents the FC region and inverted PES region. The data show that the time-dependent inversion algorithm can extract the excited electronic PES beyond the FC region until the wave packet reaches the turning point.

The FC region of the S_1 surface of the NO_2 molecule is inverted exactly because it has two kinds of resonances and is trapped temporarily in the resonance before the dissociation. However, the S_0 surface has a pronounced well and the ground state wave functions are localized around the equilib-

rium position, the amplitude of the correlation function decays quickly in exit channels. Extraction of the PES along the entire dissociation channel may be accomplished by using the PES of another known electronic state for the final state with shallow well. Another way to extract the PES along the dissociation coordinate is to use the measured mean position of atoms in the molecules by ultrafast x-ray or electron diffraction.

Discussion

The time-dependent inversion method has been applied to extract the PES of the excited electronic state from tracking the time-dependent data (*i.e.* the correlation function), which can be synthesized from the Raman excitation profile (REP) in the photodissociation process. To demonstrate the feasibility of the time-dependent inversion algorithm, we have simulated the inversion of the PES of the NO_2 molecule in the UV photodissociation process. Using the inversion algorithm and the wave packet propagation by turns, we have demonstrated that this algorithm extracts underlying PES piece by piece.

The results show that we can obtain the excited electronic PES along the dissociation path from the FC region to the exit channel as far as the propagated wave packet on the excited PES overlaps with excited vibrational states in the ground electronic state. This numerical experiment should be regarded as extremely encouraging for extracting the detailed structure of non-FC regions from frequency measurement. Because the inverse algorithm included the asymptotic condition of the exit channels in Eq. (10), it can
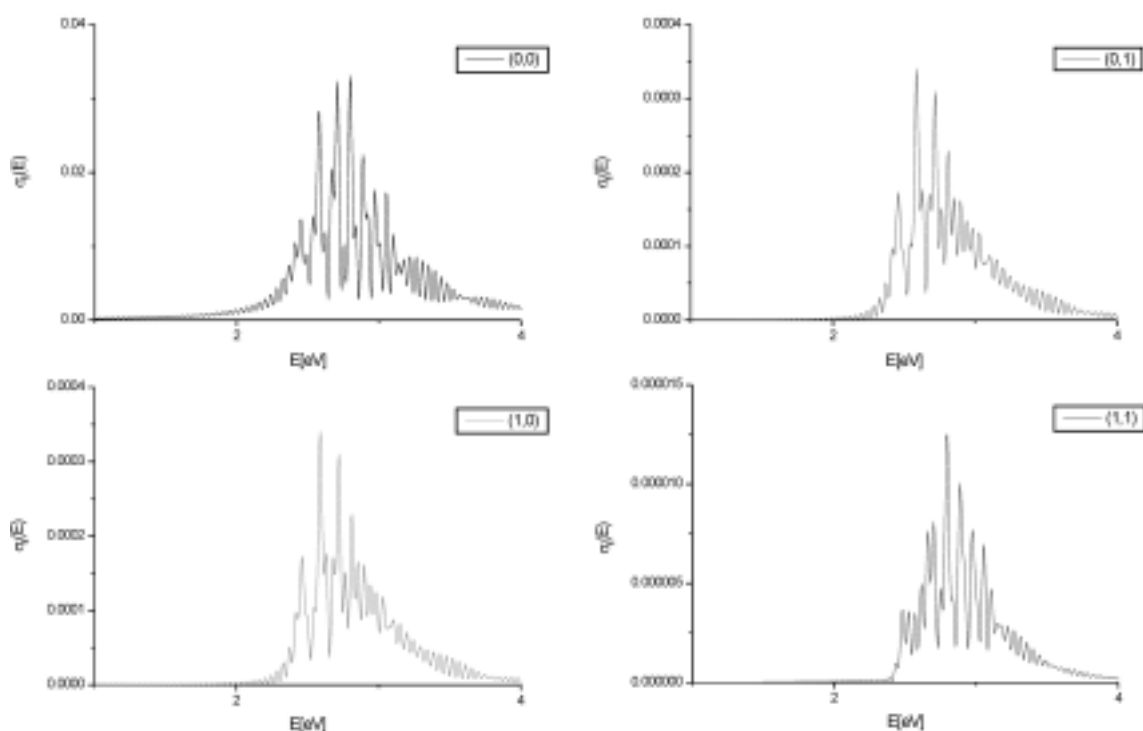

Figure 4. Raman Excitiation Profile. $\sigma_{fi}(E)$. $f = (0,0)$, $(0,1)$, $(1,0)$, $(1,1)$ ($\theta = 133.89°$).
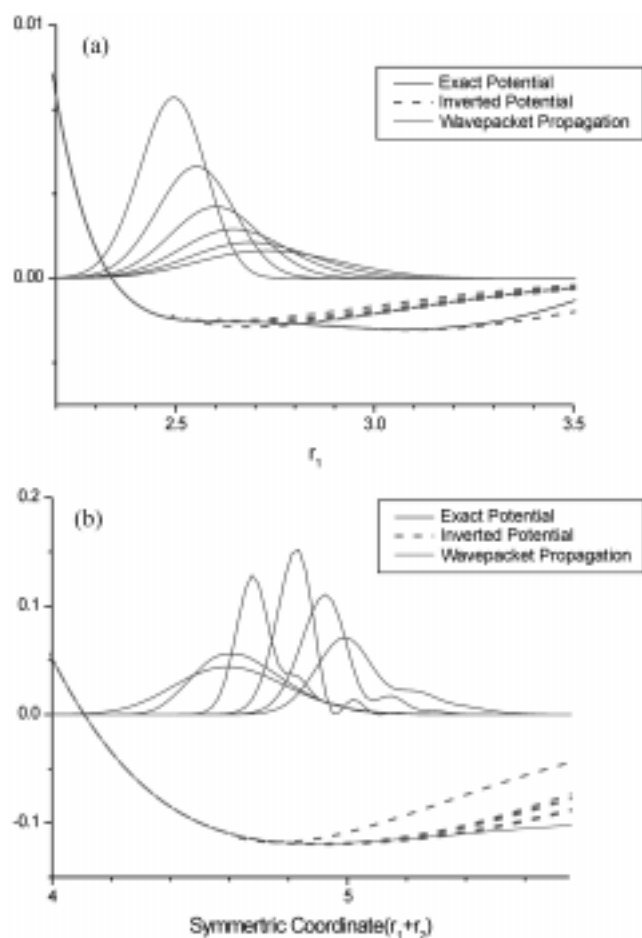
Figure 5. The comparison of the inverted potentials at a certain evolution time (0, 10, 20, 30, 40, 50 fs) with the exact one according to the wave packet propagation. (a) for a fixed value $r_2 = 2.4125$ a.u. at the equilibrium position of S_1 surface ($\theta = 133.89°$). (b) for a fixed value symmetric coordinate $r_1 - r_2 = 0$.

Table 1. FC region and Inverted PES region

	FC region	Inverted PES region
Symmetric coordinate	4.2-5	4.-5.4
r_1 (fixed $r_2 = 2.4125$ a.u.)	2.3-2.65	2.1-3.1

extract the PES smoothly without any assumption. Also, even in the case of splitting dissociation, such as NO_2[31], FNO[31,39] etc, the inversion algorithm extracts the potential beyond the FC region and the inverted potential closely resembles the exact one until the wave packet reaches the turning points in the symmetric and the asymmetric coordinates.

Compared with the time-independent inversion methods, the time-dependent tracking inversion approach has several advantages. In the time-independent method, it is necessary to assign quantum numbers to compare the experimental data with the corresponding data generated from the trial potential. The assignment process is very difficult in many situations, for example, when the potential is multidimensional and when the spectra are non-separable. However, in the tracking approach the assignment is avoided completely,

since the time carries out the assigning.

Also, the proposed tracking inversion method is a quite different approach from the fitting methods. Usually, the deviation of the fitted from the exact potentials becomes larger as the dissociation coordinates move further from the equilibrium position. But, the tracking algorithm automatically satisfies the boundary condition, avoiding the discrepancy far from the equilibrium position.

Moreover, we note that the proposed approach can be extended to extract the underlying PES and dipole functions simultaneously from tracking the mean position of wave packets. Most of the PES's can be obtained by the control of the wave packet trajectories.

References

1. Levine, R. D.; Bernstein, R. B. *Molecular Reaction Dynamics and Chemical Reactivity*; Oxford University Press: New York, 1987.
2. Buck, U. *Rev. Mod. Phys.* **1974**, *46*, 369; *Comput. Phys. Rep.* **1986**, *5*, 1.
3. Gerber, R. B. *Comments At. Mol. Phys.* **1985**, *17*, 65.
4. Buckingham, A. D.; Fowler, P. W.; Hutson, J. M. *Chem. Rev.* **1988**, *88*, 963.
5. Friesner, R. A. *Annu. Rev. Phys. Chem.* **1991**, *42*, 341.
6. Ho, T.-S.; Rabitz, H. *J. Chem. Phys.* **1988**, *89*, 5614; **1991**, *94*, 2305; **1992**, *96*, 7092; *J. Phys. Chem.* **1993**, *97*, 13447.
7. Kim, H. J.; Kim, Y. S. *J. Korean Chem. Soc.* **1996**, *40*, 20.
8. Kim, H. J.; Kim, Y. S. *Bull. Korean Chem. Soc.* **1997**, *18*, 1281.
9. Hutson, J. M. *Annu. Rev. Phys. Chem.* **1990**, *41*, 123.
10. Rydberg, R, Z. *Phys.* **1931**, *73*, 376; **1993**, *80*, 514.; Rees, A. L. G. *Proc. Phys. Soc.* **1947**, *59*, 998.
11. Roth, R. M.; Ratner, M. A.; Gerber, R. B. *Phys. Rev. Lett.* **1984**, *52*, 1288.
12. Tikhonov, A. N.; Arsenin, V. *Solution of Ill-posed Problem*; Wiley: Washington, DC, 1977.
13. Snieder, R. *Inverse Probl.* **1991**, *7*, 409.
14. Bates, H. *Inverse Scattering Problems in Optics*; Springer Verlag: Berlin, 1980.
15. Bertero, M.; Del Mol, C.; Pike, E. R. *Inverse Probl.* **1985**, *1*, 301; **1988**, *4*, 573.
16. Hansen, P. C. *Inverse Probl.* **1992**, *8*, 849; *SIAM Rev.* **1992**, *34*, 561.
17. Zewail, A. H. *Science* **1988**, *242*, 1645.
18. Bernstein, R. B.; Zewail, A. H. *J. Phys. Chem.* **1990**, *170*, 321.
19. Roberts, G.; Zewail, A. H. *J. Phys. Chem.* **1991**, *95*, 7973.
20. Zewail, A. H. *J. Phys. Chem.* **1993**, *97*, 12427.
21. Grueble, M.; Roberts, G.; Dantus, M.; Bowman, R. M.; Zewail, A. H. *Chem. Phys. Lett.* **1990**, *166*, 459.
22. Kosloff, R. *J. Phys. Chem.* **1988**, *92*, 2087.
23. Baer, R.; Kosloff, R. *J. Phys. Chem.* **1995**, *99*, 2534.
24. Lu, Z.; Rabitz, H. *Phys. Rev.* **1995**, *A52*, 1961.
25. Scoles, G.; *Atomic and Molecules Beam Methods*; Oxford University Press: New York, 1988; Vol. 1.
26. Stewart, O. W.; Imre, D. G. *J. Phys. Chem.* **1988**, *92*,

3363; **1988**, *92*, 6636.

27. Feit, M. D.; Fleck, J. A. Jr.; Steiger, A. *J. Compl. Phys.* **1982**, *47*, 412.

28. Vasan, V. S.; Cross, R. J. *J. Chem. Phys.* **1982**, 3871.

29. Mayor, F. S.; Askar, A.; Rabitz, H. A. *J. Chem. Phys.* **1999**, *111*, 2423.

30. Untch, A.; Weide, K.; Schinke, R. *J. Chem. Phys.* **1991**, *9*, 6496.

31. Huber, J. R.; Schinke, R. *J. Phys. Chem.* **1993**, *97*, 3463.

32. Manthe, U.; Meyer, H.-D.; Cederbaum, L. S. *J. Chem. Phys.* **1992**, *97*, 3199.

33. Johnson, B. R.; Kinsey, J. L. *Femtosecond Chemistry* **1994**,

354.

34. Mohan, V.; Sathyamurthy, N. *Quantal Wavepacket Calculations of Reactive Scattering* **1988**, 214.

35. McDonald, J. K.; Merritt, J. A.; Kalasinsky, V. F.; Heusel, H. L.; During, J. R. *J. Mol. Spectrosc.* **1986**, *117*, 69.

36. Schinke, R.; Novella, M.; Suter, H. O.; Huber, J. R. *J. Chem. Phys.* **1990**, *93*, 1098.

37. Hirsch, B.; Buenker, R. J. *Mol. Phys.* **1993**, *80*, 145.

38. Bruce, R. J.; William, P. R. *J. Chem. Phys.* **1986**, *85*, 4538.

39. Ogai, A.; Brandon, J.; Reisler, H.; Suter, U. H.; Huber, J. R.; Dirke, M. V.; Schinke, R. *J. Chem. Phys.* **1992**, *96*, 6643.